Momentum-Space Entanglement and Loschmidt Echo in Luttinger Liquids after a Quantum Quench

Balázs Dóra, Rex Lundgren, Mark Selover, and Frank Pollmann

Momentum-space entanglement and Loschmidt echo in Luttinger liquids after a quantum quench

Balázs Dóra,[1, *] Rex Lundgren,[2, †] Mark Selover,[2] and Frank Pollmann[3]

[1]*Department of Theoretical Physics and BME-MTA Exotic Quantum Phases Research Group,*
Budapest University of Technology and Economics, 1521 Budapest, Hungary
[2]*Department of Physics, The University of Texas at Austin, Austin, Texas 78712, USA*
[3]*Max-Planck-Institut für Physik komplexer Systeme, 01187 Dresden, Germany*
(Dated: June 14, 2016)

Luttinger liquids (LLs) arise by coupling left- and right-moving particles through interactions in one dimension. This most natural partitioning of LLs is investigated by the momentum-space entanglement after a quantum quench using analytical and numerical methods. We show that the momentum-space entanglement spectrum of a LL possesses many universal features both in equilibrium and after a quantum quench. The largest entanglement eigenvalue is identical to the Loschmidt echo, i.e. the overlap of the disentangled and final wavefunctions of the system. The second largest eigenvalue is the overlap of the first excited state of the disentangled system with zero total momentum and the final wavefunction. The entanglement gap is universal both in equilibrium and after a quantum quench. The momentum-space entanglement entropy is always extensive and saturates fast to a time independent value after the quench, in sharp contrast to a spatial bipartitioning.

PACS numbers: 05.70.Ln,71.10.Pm,03.67.Mn

Introduction. There is nothing more quantum mechanical than entanglement, when the state of certain particles cannot be described independently from the rest. This constitutes one of the most fundamental differences between classical and quantum physics. While entanglement has always been considered as an interesting quantity from its early existence, its governing role in various fields of physics, especially those fields dominated by strong correlations, has only become clear recently [1]. For example, entanglement plays an important role in understanding the thermodynamics of black holes [2], quantum information theory [3] and (topological) order [4].

The entanglement characteristics of a system is obtained usually by partitioning it into two distinct regions, and investigating the properties of the reduced density matrix (eigenvalues, entropies etc.) of one of the regions. While this partitioning is mostly spatial, i.e. done in real-space, other ways of partitioning are equally fruitful. In particular, partitioning in *momentum-space* is natural as various instabilities and phase transitions occur by coupling distinct regions in momentum-space together via interactions. For example, Cooper pairs are made of particles with opposite momentum and give rise to superconductivity. Density waves are created from electron-hole pairs with a finite wavevector difference. In one dimension, Luttinger liquids (LLs), which host many interesting phenomena such as spin-charge separation, charge fractionalization, and non-Fermi liquid behaviour, appear after coupling right- and left-moving fermions together [5, 6]. Therefore, a momentum-space partition offers a unique perspective on the structure of many-particle wavefunctions [7–20].

Parallel to these developments, non-equilibrium dynamics [21, 22] have enjoyed immense interest due to experimental advances in cold atomic gases [23]. In this context, the study of quantum quenches, i.e. time evolving a ground state wavefunction with a different Hamiltonian, is particularly challenging due to the interplay of interactions and non-equilibrium dynamics. Recently proposals have been made about measuring entanglement in cold atom systems, e.g., by using quantum switches coupled to a composite system consisting of several copies of the original many-body system [24] or using quantum interference between the copies [25].

In this work, we combine momentum-space entanglement and quantum quenches in a LL. We demonstrate that after tracing out the left-movers, the entanglement gap (EG), which is the difference between the two lowest levels of the entanglement spectrum (ES) [26], is universal in a LL *both* in equilibrium and after a quantum quench and depends only on the Luttinger parameter. We show, by using bosonization and numerical exact diagonalization on an interacting lattice model, that the largest eigenvalue of the reduced density matrix (the lowest level of the ES) is identical to the Loschmidt echo, i.e. the overlap of the ground state of the disentangled, non-interacting system and the final wavefunction of the interacting system. The Loschmidt echo is related to statistics of work done [27, 28] and the Crooks relation [29], therefore our results create a direct link between entanglement characteristics and recent developments in non-equilibrium statistical mechanics.

Tomonaga-Luttinger model. The low energy dynamics of LLs is described in terms of bosonic sound-like collective excitations, regardless to the statistics of the

original system. The Hamiltonian of the system is [5]

$$H = \sum_{q \neq 0} \omega_q b_q^\dagger b_q + \frac{g(q)}{2}[b_q b_{-q} + b_q^\dagger b_{-q}^\dagger], \qquad (1)$$

where $g(q) = g_2|q|$, with g_2 the interaction strength, and $\omega_q = v|q|$ the energy of bosonic excitations with momentum q. Starting from the non-interacting limit with $g_2 = 0$, we focus on two extreme cases of turning on interactions, adiabatically and suddenly. In the adiabatic case (which we also refer to as the equilibrium case), the system always remains in its ground state. In the case of a sudden quantum quench, the interaction strength is suddenly changed to some finite value. The final velocity of the system is $v_f = \sqrt{v^2 - g_2^2}$. One can characterize interactions by the dimensionless Luttinger parameter, K [30], which is given by $K = \sqrt{(v - g_2)/(v + g_2)}$ for Eq. (1).

The Heisenberg equation of motions, which describe the dynamics of Eq. (1), couple only pairs of q and $-q$ modes together as $b_q(t) = u_q(t)b_q + v_q^*(t)b_{-q}^+$, where all the information about interactions and time dependence is encoded in the Bogoliubov coefficients, $u_q(t)$ and $v_q(t)$, which obey the condition, $|u_q^2(t)| - |v_q^2(t)| = 1$. Their form is known for the adiabatic and sudden quench case [31]. Since Eq. (1) is quadratic in bosonic operators, its wavefunction is given by [32]

$$|\Psi(t)\rangle = e^{-i\Phi(t)} \prod_{q>0} \frac{1}{u_q^*(t)} \exp\left(\frac{v_q^*(t)}{u_q^*(t)} b_q^\dagger b_{-q}^\dagger\right) |\Psi_0\rangle, \quad (2)$$

with $\Phi(t)$ an overall phase factor and $|\Psi_0\rangle$ is the bosonic vacuum, i.e. the ground state wavefunction of the disentangled system.

Entanglement spectrum. Knowing the explicit form of the wavefunction provides us with the density matrix, $\rho = |\Psi(t)\rangle\langle\Psi(t)|$. Instead of calculating the entanglement properties by partitioning our system in real-space, we use the natural partitioning of the wavefunction in terms of right ($q > 0$) and left ($q < 0$) moving excitations and trace out all the left-movers. By expanding the exponential in Taylor series in the wavefunction, the reduced density matrix, $\rho_A(t)$, for the right-movers reads as

$$\rho_A(t) = \exp\left(\sum_{q>0} -\ln|u_q(t)|^2 + \ln\frac{|v_q(t)|^2}{|u_q(t)|^2} b_q^\dagger b_q\right). \quad (3)$$

The eigenvalues of ρ_A are immediately obtained as $P_{\{n_q\}} = \prod_{q>0} p_{n_q}(q)$, after defining the single particle eigenvalues for a given mode as $p_n(q) = |v_q(t)|^{2n} |u_q(t)|^{-2n-2}$ with n non-negative integer. The many body ES is obtained as $-\ln(P_{\{n_q\}})$.

The largest eigenvalue of ρ_A, whose logarithm is related to the single copy (or $n = \infty$ Rényi) entropy

[33, 34], is

$$P_{max} = \prod_{q>0} p_0(q) = \prod_{q>0} |u_q(t)|^{-2}. \qquad (4)$$

The right hand side of Eq. (4) is identified as the Loschmidt echo from Ref. [32] or the return probability, i.e. the overlap of the initial ground state wavefunction and the final state wavefunction, obtained through the given time evolution, as

$$P_{max} = \mathcal{L}(t) \equiv |\langle\Psi_0|\Psi(t)\rangle|^2. \qquad (5)$$

It creates a direct link between entanglement, quantum quenches [21, 22] and work statistics [27, 28] as the latter is the Fourier transform of $\mathcal{L}(t)$. This connection and its numerical verification is one of our main results.

The ground state entanglement level of the ES is $-\ln(P_{max})$. The first excited state of the ES, which is defined as the second largest eigenvalue of ρ_A, is given by $P_1 = \max_{k>0}\left[p_1(k)\prod_{q>0,q\neq k} p_0(q)\right]$. The EG (the difference between the ground state and first excited state of the ES) is $\Delta_{EG} = \ln(P_{max}) - \ln(P_1) = 2\min_{q>0} \ln|u_q(t)/v_q(t)|$, above which a continuum of many body entanglement levels occurs.

The largest eigenvalue of ρ_A is not the only entanglement level linked to the overlap of two wavefunctions. In fact, all entanglement levels can be linked to the overlap of two wavefunctions. In particular, consider a zero net momentum excited state of the initial wavefunction as $b_{k'}^\dagger b_{-k'}^\dagger|\Psi_0\rangle$. Its overlap to the final wavefunction is $p_1(k')\prod_{q>0,q\neq k'} p_0(q)$. Similarly, all other elements of the ES are obtained by creating net zero momentum boson pairs in the initial wavefunction.

Adiabatic and sudden quench. In equilibrium, all Bogoliubov coefficients are time and momentum independent and given by $|v_q(t)|^2 = (1-K)^2/4K$. Therefore, all single particle entanglement eigenvalues, $p_n(q)$, are equal and constant and the ES is flat [10, 11]. The largest eigenvalue is

$$P_{max} = \left[\frac{1}{2} + \frac{1}{4}\left(K + \frac{1}{K}\right)\right]^{-L/2\pi\alpha} \qquad (6)$$

where $1/\alpha$ is the ultraviolet cutoff [5] and L is the system size. The EG is universal, i.e. independent of the cutoff, and given by

$$\Delta_{EG} = \ln\left[\frac{(1+K)^2}{(1-K)^2}\right]. \qquad (7)$$

After a quantum quench, the Bogoliubov coefficients are time and momentum dependent and given by $|v_q(t)|^2 = \sin^2(v_f|q|t)(1 - K^2)^2/4K^2$. The largest entanglement eigenvalue saturates to the time independent

$$P_{max} = \left[\frac{1}{2} + \frac{1}{4}\left(K + \frac{1}{K}\right)\right]^{-L/\pi\alpha} \qquad (8)$$

value after a short transient time $\sim \alpha/v$. We refrain from analyzing the full time dependence of P_{max}, which has been done in Ref. [32] for the Loschmidt echo. A finite EG also persists in this case and is given by

$$\Delta_{EG} = \ln\left[\frac{(1+K^2)^2}{(1-K^2)^2}\right]. \qquad (9)$$

This EG occurs for modes with $\sin^2(v_f|q|t) = 1$. In the thermodynamic limit (TDL), for every time t, there is always a momentum state which satisfies this condition.
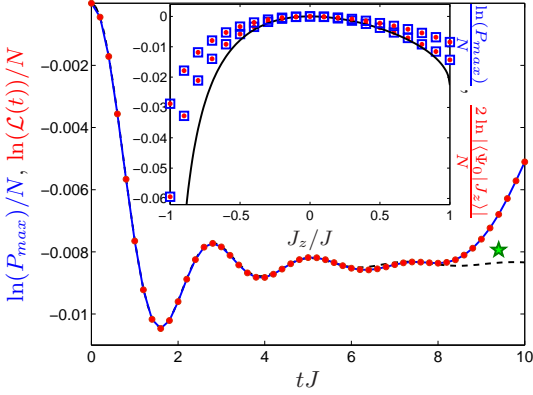

FIG. 1. (Color online) The time evolution of P_{max}, Eq. (5), (blue line) after a quantum quench for the representative case of $J_z = J/2$ and $N = 26$ is plotted, together with the overlap of the $J_z = 0$ and the quenched $J_z = J/2$ wavefunction (red circles), falling on top of each other (up to numerical accuracy). The upturn around $tJ = 9$ is due to finite size effects, following from the comparison of the infinite system result [32] (black dashed line). The green star denotes the prediction of Eq. (8), which is valid for times much larger than the transient time. The inset visualizes adiabatic results for P_{max} (blue squares) and the overlap of the ground state wavefunctions (red dots) for $N = 14$ (upper dataset) and 22 (lower dataset). The ED data approaches Eq. (6) (black line), which is valid in the TDL, upon increasing the system size.

Exact diagonalization. We now test these analytical predictions numerically using exact diagonalization (ED) on a half-filled tight binding chain of one-dimensional spinless fermions with nearest-neighbour interactions and periodic boundary conditions [5, 6]. In momentum-space, the Hamiltonian we consider is

$$H = J\sum_k \cos(k)c_k^\dagger c_k + \frac{J_z}{N}\sum_{k,p,q}\cos(q)c_{p-q}^\dagger c_p c_{k+q}^\dagger c_k, \qquad (10)$$

where c's are fermionic annihilation operators in momentum-space, N the number of lattice sites and $k = 2\pi m/N$, $n = 1\ldots N$. Its low energy physics is accounted for by Eq. (1) with $K = \pi/2[\pi - \arccos(J_z/J)]$, covering $1/2(J_z = J) < K < \infty(J_z = -J)$ [5]. [35] We consider system sizes of $N = 10, 14, 18, 22$ and 26 (to avoid a degenerate Fermi sea) and then perform finite size

scaling to reach the TDL. For the range of parameters we consider, there is a unique non-degenerate ground state. We compute the time evolution of the momentum-space wavefunction using the Krylov method until $tJ = 20$ [36]. After constructing the density matrix from the wavefunction in momentum-space basis, all left-movers (i.e. $k < 0$ modes) are traced out, giving the reduced density matrix.
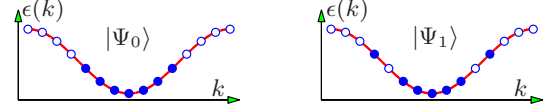

FIG. 2. (Color online) Schematic picture of the ground (left) and first excited (right) state of the half filled tight binding model with zero total momentum is visualized in momentum-space ($\epsilon(k) = J\cos(k)$), whose overlap with the final wavefunction yields the first two entanglement eigenvalues.

Eqs. (4) and (5) predict that the largest eigenvalue of ρ_A is equal to the overlap of the decoupled and coupled wavefunction. Using ED, P_{max}, as well as the overlap of the $J_z = 0$ ground state wavefunction with the finite J_z adiabatic or sudden quench wavefunction, are evaluated and shown in Fig. 1. These agree perfectly both in equilibrium and after the quench (within numerical accuracy), thus confirming the bosonization prediction. The $L/\pi\alpha$ factor in Eqs. (6) and (8) contains the short distance cutoff. The short distance cutoff is estimated from the fidelity susceptibility χ_f [32], which gives $L/2\pi\alpha \approx N\chi_f\pi^2$ with $\chi_f \approx 0.0195$ [37]. Eq. (5) also works at the $J_z = -J$ point (not shown), which falls outside of the validity of bosonization because the excitation spectrum changes from linear to quadratic in momentum. We conjecture that Eq. (5) is valid for other systems as well. We have numerically checked this conjecture on other systems [38], including the non-integrable extension (by adding second nearest neighbour hopping [39, 40]) of Eq. (10), and different boundary conditions with affirmative conclusion.

From the analysis of the the numerical data (not shown), we find that for all system sizes considered and within the critical region, the second largest eigenvalue of ρ_A equals the overlap between the final, coupled wavefunction and the first excited state of the disentangled wavefunction with total momentum 0, arising from annihilating a left and a right mover from right below the filled Fermi sea and creating a left and right mover right above the Fermi sea, shown in Fig. 2, i.e. $P_1 = |\langle\Psi_1|\Psi(t)\rangle|^2$. The numerical data for P_1 is in excellent agreement with the bosonization prediction. In the case of a quantum quench, P_1 (during its time evolution) is equal to the overlap between the time evolved wavefunction and a general total momentum zero excited state of the initial disentangled Hamiltonian, but *not necessarily* the first zero momentum excited state. However, the minimal value of P_1 over time, which defines the EG,

occurs for the first zero momentum excited state.

The EG, which is the minimal difference between the ground state and first excited state of the ES, is shown in Fig. 3. After a quantum quench, the EG is obtained from the difference of the first two eigenvalues of ρ_A after the transient time but before the revival time N/J, when finite size effects become important. The EG is largely insensitive to variations within this window. The same results are obtained when the EG is calculated from the overlaps of the final wavefunction with the states shown in Fig. 2. Around the non-interacting XX point, $\Delta_{EG} \sim -\ln(J_z^2)$ since the left and right moving fermions are perfectly disentangled in this case. Both in equilibrium and after the quantum quench, the EG is universal and in near perfect agreement with bosonization prediction throughout the critical region, depending only on K. The EG stays finite for $J_z > 0$ within the LL phase, and does not vanish even at the BKT transition point at $J_z = J$. On the other hand, the EG collapses at $J_z = -J$, signaling the first order quantum critical point. In equilibrium, $\Delta_{EG} \sim \sqrt{J_z + J}$ for $J_z \gtrsim -J$, which changes to $\Delta_{EG} \sim J_z + J$ after a quantum quench. We suspect that the EG is sensitive to any finite order quantum critical point, except possibly for the BKT transition, being of infinite order. The detection of the BKT transition is also difficult using the fidelity susceptibility [37]. One possible scenario is that the EG does not detect the BKT transition due to the non-universality of the ES [41]. In fact, recent numerical work on the momentum-space ES of the XXZ spin-half chain strongly suggests that EG (in equilibrium) remains open in the gapped phase [11]. We leave the non-universality of the ES after a quantum quench an open question.

Entanglement entropy. The amount of entanglement is quantified by the (von-Neumann or Rényi) entanglement entropy. The momentum-space von-Neumann entanglement entropy is

$$S = 2 \sum_{q>0} |u_q(t)|^2 \ln |u_q(t)| - |v_q(t)|^2 \ln |v_q(t)| \qquad (11)$$

from bosonization, and the Bogoliubov coefficients encode the properties of the final wavefunction. For a spatial bipartition, $S \sim \ln(N)$ and $\sim t$ in equilibrium and after a quench for a LL, respectively [1]. For the present case, interactions connects q and $-q$ states, and by halving momentum-space for partitioning, the number of bonds we cut through is proportional to the number of momentum states, i.e. $\sim N$. Thus, a volume law holds for the entropy both in equilibrium and after the quench. By inspecting Eq. (11), S grows as $\sim Lt^2 \ln(1/t)$ initially after the quench, before saturating (within a timescale α/v or $1/J$) to a finite, $\sim L$ but t independent value in the TDL. These results are reproduced by ED. Fig. (3) shows the ratio of the entropies (in steady state) after a quantum quench and in equilibrium from ED, free from the extensive N or L/α prefactor.
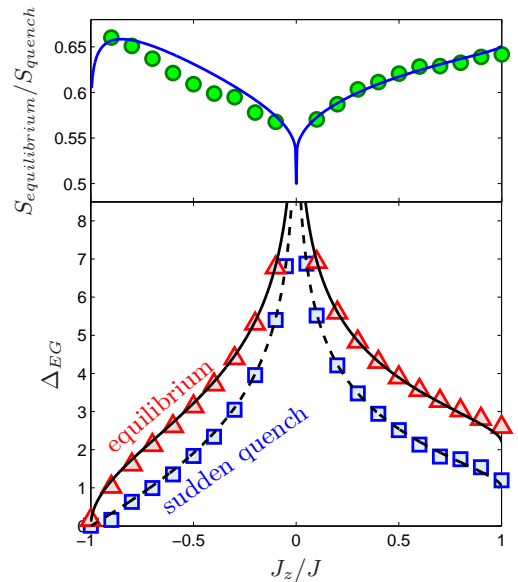

FIG. 3. (Color online) Lower panel: The EG extrapolated to the TDL in equilibrium (red triangles) and after a quench (blue squares). The black solid and dashed lines depict the analytical results without any fitting parameter from Eqs. (7) and (9), respectively. Upper panel: The ratio (circles) of the von-Neumann entanglement entropies in the steady state after the quench and in equilibrium from ED, extrapolated to the TDL, compared to the Luttinger model result (solid line) from Eq. (11), without any fitting.

We see that $S_{quench} > S_{equilibrium}$ (after a short initial transient time) and their biggest ratio is 2. This ratio is reached as one approaches the non-interacting limit.

Discussion. We have demonstrated that the low lying entanglement levels of LLs are identical to the overlap of the final wavefunction and the zero total momentum eigenstates of the disentangled Hamiltonian. The EG persists throughout the critical phase and is a universal function of the Luttinger parameter both in equilibrium and after a quantum quench. Our results create a unique link between entanglement and the Loschmidt echo [28] as well as the closely related work statistics [27]. We note our approach also quantifies the entanglement between the up and down spins in the spin filtered helical edge state of a quantum spin-Hall insulator [42].

The momentum-space entanglement entropy is always extensive, and grows initially as $S \sim Lt^2 \ln(1/t)$ after a quantum quench, before saturating to a time independent value. Understanding momentum-space entanglement bears relevance for the development of momentum-space numerical techniques built on optimally entangled states [14, 43]. The similar magnitude of the entanglement entropies in equilibrium and after quench as well as the separation of entanglement scales, i.e. the EG, near the critical point could help improve the density matrix renormalization group algorithm [11, 14]. For example, the EG seems to stay finite at the BKT tran-

sition point even after the quench, facilitating numerics [11]. Our work also present alternatives to measuring the entanglement[25] through the Loschmidt echo.

* dora@eik.bme.hu
† rexlund@physics.utexas.edu

[1] J. Eisert, M. Cramer, and M. B. Plenio, *Colloquium : Area laws for the entanglement entropy*, Rev. Mod. Phys. **82**, 277 (2010).

[2] M. Srednicki, *Entropy and area*, Phys. Rev. Lett. **71**, 666 (1993).

[3] M. Nielsen and I. Chuang, *Quantum Computation and Quantum Information* (Cambridge University Press, Cambridge, 2000).

[4] L. Amico, R. Fazio, A. Osterloh, and V. Vedral, *Entanglement in many-body systems*, Rev. Mod. Phys. **80**, 517 (2008).

[5] T. Giamarchi, *Quantum Physics in One Dimension* (Oxford University Press, Oxford, 2004).

[6] A. O. Gogolin, A. A. Nersesyan, and A. M. Tsvelik, *Bosonization and Strongly Correlated Systems* (Cambridge University Press, Cambridge, 1998).

[7] R. Thomale, D. P. Arovas, and B. A. Bernevig, *Nonlocal order in gapless systems: Entanglement spectrum in spin chains*, Phys. Rev. Lett. **105**, 116805 (2010).

[8] X.-L. Qi, H. Katsura, and A. W. W. Ludwig, *General relationship between the entanglement spectrum and the edge state spectrum of topological quantum states*, Phys. Rev. Lett. **108**, 196402 (2012).

[9] R. Lundgren, V. Chua, and G. A. Fiete, *Entanglement entropy and spectra of the one-dimensional kugel-khomskii model*, Phys. Rev. B **86**, 224422 (2012).

[10] R. Lundgren, Y. Fuji, S. Furukawa, and M. Oshikawa, *Entanglement spectra between coupled tomonaga-luttinger liquids: Applications to ladder systems and topological phases*, Phys. Rev. B **88**, 245137 (2013).

[11] R. Lundgren, J. Blair, M. Greiter, A. Läuchli, G. A. Fiete, and R. Thomale, *Momentum-space entanglement spectrum of bosons and fermions with interactions*, Phys. Rev. Lett. **113**, 256404 (2014).

[12] R. Lundgren, *Momentum-space entanglement in heisenberg spin-half ladders*, Phys. Rev. B **93**, 125107 (2016).

[13] R. Lundgren, J. Blair, P. Laurell, N. Regnault, G. A. Fiete, M. Greiter, and R. Thomale, *Universal entanglement spectra in critical spin chains*, arXiv:1512.09030.

[14] G. Ehlers, J. Sólyom, O. Legeza, and R. M. Noack, *Entanglement structure of the hubbard model in momentum space*, Phys. Rev. B **92**, 235116 (2015).

[15] I. Mondragon-Shem, M. Khan, and T. L. Hughes, *Characterizing disordered fermion systems using the momentum-space entanglement spectrum*, Phys. Rev. Lett. **110**, 046806 (2013).

[16] E. C. Andrade, M. Steudtner, and M. Vojta, *Anderson localization and momentum-space entanglement*, Journal of Statistical Mechanics: Theory and Experiment **2014**, P07022 (2014).

[17] V. Balasubramanian, M. B. McDermott, and M. Van Raamsdonk, *Momentum-space entanglement and renormalization in quantum field theory*, Phys. Rev. D **86**, 045014 (2012).

[18] L. A. Pando Zayas and N. Quiroz, *Left-right entanglement entropy of boundary states*, Journal of High Energy Physics **2015**, 1 (2015).

[19] D. Das and S. Datta, *Universal features of left-right entanglement entropy*, Phys. Rev. Lett. **115**, 131602 (2015).

[20] M.-C. Chung, A. Iucci, and M. A. Cazalilla, *Thermalization in systems with bipartite eigenmode entanglement*, New J. Phys. **14**, 075013 (2012).

[21] A. Polkovnikov, K. Sengupta, A. Silva, and M. Vengalattore, *Colloquium : Nonequilibrium dynamics of closed interacting quantum systems*, Rev. Mod. Phys. **83**, 863 (2011).

[22] J. Dziarmaga, *Dynamics of a quantum phase transition and relaxation to a steady state*, Adv. Phys. **59**, 1063 (2010).

[23] I. Bloch, J. Dalibard, and W. Zwerger, *Many-body physics with ultracold gases*, Rev. Mod. Phys. **80**, 885 (2008).

[24] D. A. Abanin and E. Demler, *Measuring entanglement entropy of a generic many-body system with a quantum switch*, Phys. Rev. Lett. **109**, 020504 (2012).

[25] R. Islam, R. Ma, P. M. Preiss, M. E. Tai, A. Lukin, M. Rispoli, and M. Greiner, *Measuring entanglement entropy in a quantum many-body system*, Nature **528**, 77 (2015).

[26] H. Li and F. D. M. Haldane, *Entanglement spectrum as a generalization of entanglement entropy: Identification of topological order in non-abelian fractional quantum hall effect states*, Phys. Rev. Lett. **101**, 010504 (2008).

[27] M. Campisi, P. Hänggi, and P. Talkner, *Colloquium : Quantum fluctuation relations: Foundations and applications*, Rev. Mod. Phys. **83**, 771 (2011).

[28] A. Silva, *Statistics of the work done on a quantum critical system by quenching a control parameter*, Phys. Rev. Lett. **101**, 120603 (2008).

[29] G. E. Crooks, *Entropy production fluctuation theorem and the nonequilibrium work relation for free energy differences*, Phys. Rev. E **60**, 2721 (1999).

[30] $K = 1$ for the non-interacting case, and $K \gtrless 1$ for attraction/repulsion, respectively.

[31] A. Iucci and M. A. Cazalilla, *Quantum quench dynamics of the luttinger model*, Phys. Rev. A **80**, 063619 (2009).

[32] B. Dóra, F. Pollmann, J. Fortágh, and G. Zaránd, *Loschmidt echo and the many-body orthogonality catastrophe in a qubit-coupled luttinger liquid*, Phys. Rev. Lett. **111**, 046402 (2013).

[33] I. Peschel and J. Zhao, *On single-copy entanglement*, J. Stat. Mech. p. P11002 (2005).

[34] J. Eisert and M. Cramer, *Single-copy entanglement in critical quantum spin chains*, Phys. Rev. A **72**, 042112 (2005).

[35] By a momentum-space Jordan-Wigner transformation, we arrive at a momentum-space Hamiltonian of hardcore bosons, which is solved numerically using ED or the Lanczos method.

[36] Y. Saad, *Analysis of some krylov subspace approximations to the matrix exponential operator*, SIAM Journal

on Numerical Analysis **29**, 209 (1992).

[37] J. Sirker, *Finite-temperature fidelity susceptibility for one-dimensional quantum systems*, Phys. Rev. Lett. **105**, 117203 (2010).

[38] See EPAPS Document No. XXX for supplementary material providing further analysis on other models.

[39] S. Mukerjee and B. S. Shastry, *Signatures of diffusion and ballistic transport in the stiffness, dynamical correlation functions, and statistics of one-dimensional systems*, Phys. Rev. B **77**, 245131 (2008).

[40] C. Bartsch and J. Gemmer, *Boltzmann-type approach to transport in weakly interacting one-dimensional*

fermionic systems, Phys. Rev. E **85**, 041103 (2012).

[41] A. Chandran, V. Khemani, and S. L. Sondhi, *How universal is the entanglement spectrum?*, Phys. Rev. Lett. **113**, 060501 (2014).

[42] C. Wu, B. A. Bernevig, and S.-C. Zhang, *Helical liquid and the edge of quantum spin hall systems*, Phys. Rev. Lett. **96**, 106401 (2006).

[43] J. Motruk, M. P. Zaletel, R. S. K. Mong, and F. Pollmann, *Density matrix renormalization group on a cylinder in mixed real and momentum space*, Phys. Rev. B **93**, 155139 (2016).